Journal of The Electrochemical Society, **152** (1) A158-A163 (2005)
0013-4651/2004/152(1)/A158/6/$7.00 © The Electrochemical Society, Inc.

Effect of Counter Ion Placement on Conductivity in Single-Ion Conducting Block Copolymer Electrolytes

Sang-Woog Ryu, Patrick E. Trapa,* Solar C. Olugebefola, Juan A. Gonzalez-Leon, Donald R. Sadoway,* and Anne M. Mayes*,z

Department of Materials Science and Engineering, Massachusetts Institute of Technology, Cambridge, Massachusetts 02139-4307, USA

Single-ion conducting block copolymer electrolytes were prepared in which counter ions were tethered to the polymer backbone to achieve a lithium transference number of unity. Through tailored anionic synthesis, the influence of counter ion placement on conductivity was investigated. Incorporating the anions outside the ion-conducting [poly(ethylene oxide)-based] block, such as in poly(lauryl methacrylate)-*block*-poly(lithium methacrylate)-*block*-poly[(oxyethylene)$_9$ methacrylate], known as PLMA-*b*-PLiMA-*b*-POEM, and P(LMA-*r*-LiMA)-*b*-POEM, caused lithium ions to dissociate from the carboxylate counter ions upon microphase separation of the POEM and PLMA blocks, yielding conductivities of 10^{-5} S/cm at 70°C. In contrast, incorporating anions into the conducting block, as in PLMA-*b*-P(LiMA-*r*-OEM), rendered the majority of lithium ions immobile, resulting in conductivities one to two orders of magnitude lower over the range of temperatures studied for equivalent stoichiometries. Converting the carboxylate anion to one that effectively delocalized charge through complexation with the Lewis acid BF_3 raised the conductivity of the latter system to values comparable to those of the other electrolyte architectures. Ion dissociation could thus be equivalently achieved by using a low charge density counter ion ($COOBF_3^-$) or by spatially isolating the counter ion from the ion-conducting domains by microphase separation.
 [DOI: 10.1149/1.1828244]

Manuscript submitted April 9, 2004; revised manuscript received June 11, 2004. Available electronically December 2, 2004.

In the arena of possible advancements in lithium rechargeable batteries, the case for a solid polymer electrolyte is compelling. Such materials offer the promise of simplified processing, better temperature stability, thinner cells, flexible geometries, and enhanced safety.[1] Most solid polymer electrolyte research has focused on increasing the conductivity of such systems while still maintaining good thermal, electrochemical, and mechanical stability. However, ultimately, the room temperature conductivity for various dry polymer electrolytes plateaus at $\sim 10^{-4}$ S/cm when using lithium bis(trifluoromethanesulfonyl) imide salt.[1,2] This is not surprising given that most such systems incorporate amorphous poly(ethylene oxide) (PEO).

To make further performance gains, the transference number of the electrolyte assumes great importance, especially as the drain rate of the battery is increased. When a battery is subjected to high discharge rates, a gradient in salt concentration is formed, with ion accumulation occurring at the anode and depletion regions forming within the composite cathode.[3,4] Such gradients change both the lithium diffusion coefficient and the density of charge carriers across the electrolyte.[5] The dc conductivity falls well below the initial ac value, leading to polarization through IR drop, a factor that reduces the capacity of the battery by narrowing the voltage window seen by the electrodes. This problem largely disappears when the electrolyte's transference number is unity.

Single-ion conducting polymer electrolytes for lithium batteries have already received much attention.[6-15] One issue confronting researchers is how to retain high cation mobility upon tethering the anion to the polymer. In such systems, ion pairing interactions can render lithium ions relatively immobile, leading to low conductivity. Alternative approaches to single-ion conductors include the use of a bulky oligo/polymeric counter ion[16,17] or the creation of anion trap sites[18,19] within the electrolyte. The conductivity of these systems is good, but the lithium transference number falls well short of unity, thus nullifying some advantages of a truly fixed-anion electrolyte.[3]

The success of single-ion conducting polymer electrolytes hinges upon finding a way to promote charge dissociation, thereby enhancing Li^+ mobility. One approach is to employ bulky, low charge density anions by complexing tethered anions with a Lewis acid.[12-14] For example, Florjanczyk *et al.* reported significant enhancements in the conductivity of single-ion conducting gel polymer electrolytes by incorporating BF_3, which complexed with the carboxylate anions of the polymer network.[13]

Here we explore an alternate strategy to promote ion dissociation by spatially isolating the anions in a secondary phase of the polymer electrolyte. Placement of the counter ions within the electrolyte is controlled by anionic synthesis of single-ion conducting block copolymer electrolytes (BCEs)[20-22] incorporating the incompatible block components poly(lauryl methacrylate), known as PLMA, and poly((oxyethylene)$_9$ methacrylate), known as POEM.[20] To provide charge carriers, lithium methacrylate is added into the backbone in three distinct molecular architectures: randomly within the hydrophilic block, P(LiMA-*r*-POEM), randomly within the hydrophobic block, P(LMA-*r*-LiMA), or as a separate block, PLiMA, sandwiched between PLMA and POEM. For the two architectures in which the LiMA is incorporated outside the ion-conducting (POEM) block, microphase separation appears to promote dissociation of Li^+ from the carboxylate anions, resulting in conductivities one to two orders of magnitude above the counterpart structure in which LiMA resides in the POEM domain. The effect of counter ion spatial isolation on ion dissociation is shown to be comparable to that of lowering the anion charge density through the addition of BF_3.

Experimental

Anionic methods were used to prepare single-ion conducting BCEs containing lithium methacrylate (LiMA), lauryl methacrylate (LMA) and (oxyethylene)$_9$ methacrylate (OEM) in different molecular architectures. All reagents used in this study were purchased from Aldrich. Tetrahydrofuran (THF) was rigorously purified by refluxing over sodium/benzophenone for 48 h, and then distilled in a nitrogen atmosphere just prior to use. Both *tert*-butyl methacrylate (tBMA) and LMA were distilled over CaH_2 and then again over trioctylaluminum (10 mol %). OEM, $M_n = 475$ g/mol, was stirred over CaH_2 for 2 days before being passed through an alumina column and diluted with freshly distilled THF to a 1:1 volume ratio in a dry nitrogen atmosphere. *sec*-Butyllithium (*s*-BuLi), trimethylsilylchloride [$(CH_3)_3SiCl$], sodium iodide (NaI), chloroform, acetonitrile, and methanol were used as received. 1,1-Diphenylethylene (DPE) was vacuum distilled in the presence of *s*-BuLi (3 mol %). Lithium chloride (LiCl) was dried under vacuum at 200°C for 48 h.

The anionic block copolymerization was carried out by sequential addition of monomers to a sealed glass reactor fitted with silicone rubber septa. LiCl (5 times excess to initiator), DPE (1.2 times

* Electrochemical Society Active Member.
z E-mail: amayes@mit.edu

Table I. Molecular characteristics of block copolymer precursors.

	Composition		Molecular weight (g/mol)	Polydispersity (M_w/M_n)
	(Wt %)	(Mol %)		
PLMA-*b*-PtBMA-*b*-POEM	28:11:61	30:35:35	28,900	1.22
PLMA-*b*-PtBMA-*b*-POEM	18:05:77	24:20:56	83,800	1.16
P(LMA-*r*-tBMA)-*b*-POEM	28:10:62	31:33:36	32,800	1.17
P(LMA-*r*-tBMA)-*b*-POEM	11:06:83	15:24:61	44,300	1.16
PLMA-*b*-P(tBMA-*r*-OEM)	31:09:60	34:30:36	41,800	1.20

excess to initiator), and THF were introduced into the reactor and submitted to several nitrogen/vacuum pump-purge cycles. After cooling to −78°C, a few drops of *s*-BuLi were added via syringe until the solution became pale orange. The calculated amount of *s*-BuLi was then introduced and stirred for 30 min. The purified first monomer was then added to the initiator solution, prompting the solution to change color from red to pale yellow. An aliquot of polymer solution was taken after 3 h of reaction time and deactivated with methanol. To the remaining reaction medium, the second monomer was added, and the solution was allowed to stir for 3 h. For the triblock copolymers, these procedures were repeated for the addition of the third block. The polymerization was then terminated with methanol, and the solution was poured into a large excess of hexane to precipitate the polymer. To remove residual LiCl, the polymer was dissolved in benzene and passed through an alumina column, then freeze-dried for 8 h. The M_n values were determined by proton nuclear magnetic resonance (^{1}H NMR, Bruker DPX in $CDCl_3$) using characteristic resonances at 4.1 ppm ($COO—CH_2$, POEM), 3.9 ppm ($COO—CH_2$, PLMA), and 1.4 ppm [$C—(CH_3)_3$, PtBMA], and comparing with CH_3 proton resonances of the *s*-Bu initiator residue at 0.6-0.8 ppm. Molecular weight distributions of the synthesized polymers were determined at 30°C by gel permeation chromatography (Viscotek GPCmax) using polystyrene standard samples as a reference and THF as a carrier solvent.

Hydrolysis of PtBMA to poly(methacrylic acid) was carried out with 1.2 times excess of $(CH_3)_3SiCl$-NaI in a mixed solvent of acetonitrile and chloroform (3/5, v/v) at 25°C for 30 min. After complete drying, the polymer was dissolved again in THF and poured into water containing trace amounts of sodium thiosulfate. The precipitated polymer was then recovered by centrifuge, reprecipitated in hexane, and dried in a vacuum oven at 100°C for 2 days. The reaction was confirmed by the disappearance of the characteristic resonance of *tert*-butyl protons of the parent polymer at 1.4 ppm using ^{1}H NMR analysis. The hydrolyzed block copolymer was then dissolved in methanol/THF (2/1, v/v), and a quantitative amount of lithium methoxide was added slowly to the solution at room temperature. After a pH of 7 was reached, the solution was poured into 3:1 (v/v) petroleum ether/ethanol mixed solvent, and the precipitated polymer was dried under vacuum at 100°C for 3 days. BF_3 incorporation was carried out in methanol under a nitrogen atmosphere. BF_3-THF complex was introduced to a 5 wt % polymer solution to achieve a 1:1 molar ratio $BF_3:COO^-$. After 3 h stirring at 25°C, the solvent was removed by evaporation and the obtained polymer dried under vacuum at 100°C for 3 days.

For electrochemical studies, the dried polymer was redissolved in chloroform or THF, solvent cast onto glass substrates and dried under vacuum at 100°C for 3 days. The obtained polymer film (300-500 μm thick) was then cut into pieces of ~0.1 cm^2 area in a glove box.

Small angle neutron scattering (SANS) experiments were carried out at room temperature on the NG-7 30-m instrument of the Cold Neutron Research Facility at the National Institute of Standards and Technology (NIST) to investigate the morphology of the block copolymers. A sample-to-detector distance of 9 m and a monochromated neutron wavelength of 6 Å were used to cover scattering wavevectors in the range of $0.002\ Å^{-1} < Q < 0.07\ Å^{-1}$.

Atomic force microscopy (AFM) was performed on a Digital Instruments (Santa Barbara, CA) Nanoscope IIIa scanning probe microscope with a TAP300 silicon cantilever (Nano Devices) having a spring constant of ~40 N/m. A film ~200 nm thick of P(LMA-*r*-LiMA)-*b*-POEM was spin-coated from the THF solution onto a cleaned Si substrate. A phase image of the BCE film was recorded in tapping mode.

Fourier transform infrared (FTIR) spectra were measured using a Magna-IR 860 spectrometer (Thermo-Nicolet) with an 80° specular reflectance accessory. Samples were solvent cast onto silicon substrates and placed under vacuum overnight to remove moisture.

Differential scanning calorimetry (DSC) measurements were carried out on a TA Instruments Q100 at a heating rate of 20°C/min. Samples were solution cast into standard aluminum pans. The samples were thermally cycled until no sign of residual moisture was observed. Glass transition values are reported from the last heating scan.

Electrical conductivities were determined by impedance spectroscopy using a waveform generator/response analyzer (Solartron model 1260 frequency response analyzer, Solartron Analytical, Houston, TX) controlled by a personal computer running commercially available software (Z60, Scribner Associates, Inc., Southern Pines, NC). The test fixture consisted of two blocking electrodes made of stainless steel and attached to a micrometer that measured the electrode separation and, hence, the thickness of the polymer specimen, which was kept under an atmosphere of flowing argon gas.

Lithium symmetric cells fitted with the polymer electrolytes (300-500 μm thick, ~0.1 cm^2 area) were used to obtain a measure of the lithium transference number. The electrodes were active to lithium ions but blocked the anions; upon application of a stepped potential, the initial current (I_0) reflected both cation and counter ion contributions, whereas the long-term, steady-state value (I_{ss}) arose solely from lithium ion motion. The transference number was then taken to be I_0/I_{ss}. This simplified method does not take into account the concentration dependence of the lithium diffusion coefficient,[23] nor does it correct for any changes in the IR drop across electrode surface films (either due to a variation in current or in film thickness during the course of the test[24]). However, these added complications have no effect if the transference number is experimentally found to be unity; a constant current response obviates the need for IR corrections and also implies that concentration gradients are absent in the electrolyte. Transference number tests were performed at room temperature.

The electrochemical stability of the materials was investigated by cyclic voltammetry performed at room temperature. The electrolyte was pressed between an oversized counter electrode of lithium and a 0.08 cm^2 working electrode of platinum to a film thickness of approximately 200 μm. Using a Solartron 1286 electrochemical interface (Solartron Analytical, Houston, TX) controlled by a personal computer running CorrWare (Scribner Associates, Inc., Southern Pines, NC), the potential was scanned from +2.5 to +5.0 V at a sweep rate of 25 mV s^{-1}.

Results and Discussion

The molecular weight and compositional characteristics of the precursor block copolymers synthesized for this study are presented

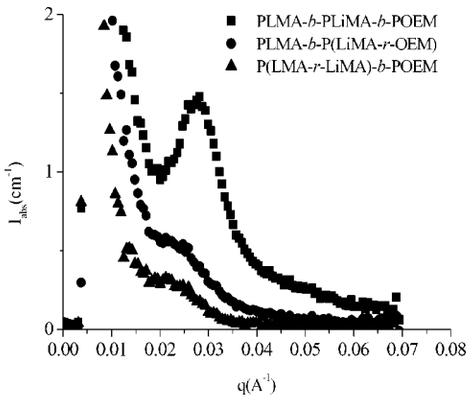

Figure 1. SANS data for three single-ion conducting BCEs with 1:1:1 molar ratios LMA:LiMA:OEM. The domain spacing calculated from the scattering maximum for the triblock system is 22.7 nm as compared to ~28.5 nm for the two diblocks.

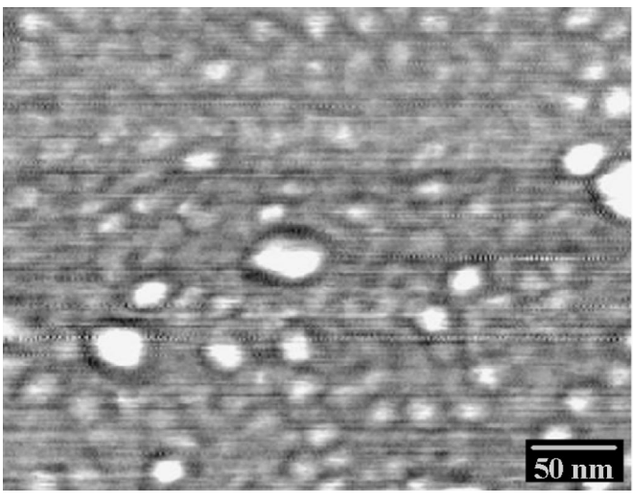

Figure 2. Phase-contrast AFM image of P(LMA-*r*-LiMA)-*b*-POEM (1:1:1) film cast on silicon. The majority POEM domains (62 wt %) appear as the darker phase.

in Table I. For the diblock architectures, monomer mixtures of LMA/tBMA or OEM/tBMA were polymerized first, followed by sequential addition of OEM or LMA monomer, respectively. Polymerization of the triblock materials was carried out by sequential addition of LMA, tBMA, and OEM. In all experiments, monomer conversions were almost quantitative based on gravimetric analysis; the molecular weight and composition of the block copolymers were controlled by the feed ratio. Molecular weights of the block copolymer products ranged from 28,900 to 83,800 g/mol, with somewhat broad polydispersities (~1.2), indicating partial termination of the first block from impurities in the OEM macromonomer. Hydrolysis of the tBMA component and subsequent lithiation produced single-ion conducting BCEs.

Previously, achieving high conductivity in salt-doped BCEs required microphase separation (local demixing) of the ion-conducting and secondary blocks.[20,21] Evidence for microphase separation of the single-ion conducting BCEs was obtained from SANS, AFM, and DSC studies. SANS data from PLMA-*b*-PLiMA-*b*-POEM, P(LMA-*r*-LiMA)-*b*-POEM, and PLMA-*b*-P(LiMA-*r*-OEM) systems, each with 1:1:1 ratio LMA:LiMA:OEM, are shown in Fig. 1. For the triblock (PLMA-*b*-PLiMA-*b*-POEM), an intense first-order reflection is observed at a wavevector $q^* = 0.0277$ Å^{-1}, indicating that this material is ordered (microphase separated), with a characteristic period of ~22.7 nm.

Peaks are also observed for the diblock materials, but they are less intense and shifted to lower wavevectors. The latter finding is consistent with the higher molecular weight of these systems compared with the triblock (Table I). The lower peak intensities can be explained by the lower scattering contrast between the distinct blocks of these systems. Table II shows the calculated neutron scattering length densities for each of the block components of the BCEs investigated. Block miscibility in the PLMA-*b*-P(LiMA-*r*-OEM) system is unlikely due to the difference in block polarities. The higher peak intensity of the PLMA-*b*-PLiMA-*b*-POEM triblock compared with PLMA-*b*-P(LiMA-*r*-OEM) suggests that the three blocks organize as three distinct domains, creating high contrast between the PLiMA and PLMA phases (see Table II). For P(LMA-*r*-LiMA)-*b*-POEM, the calculated scattering length densities predict very weak scattering contrast between the blocks. Observation of a peak at wavevector $q^* = 0.022$ Å^{-1} ($d = 28.5$ nm) is thus good evidence of block demixing in this system.

Table II. Neutron scattering length densities for BCE components.

Block components[a]	b_v (Å^{-2})
POEM	0.697×10^{-6}
PLiMA	1.267×10^{-6}
PLMA	0.151×10^{-6}
P(LiMA-*r*-OEM)	0.982×10^{-6}
P(LMA-*r*-LiMA)	0.709×10^{-6}

[a] Calculations assume a mass density of 1.1 g/cm^3.

Further support for this conclusion was obtained from AFM investigation of a P(LMA-*r*-LiMA)-*b*-POEM (1:1:1) block copolymer film deposited on silicon. Figure 2 shows a phase image of the film surface. The contrast in this case arises from differences in stiffness exhibited across the surface.[25,26] Two distinct phases are seen with a characteristic periodicity of ~25 nm, which is smaller than, but still consistent with, the value determined by SANS (~28.5 nm). In this image, the light phase is interpreted to be the stiffer minority P(LMA-*r*-LiMA) block domains, whereas the majority POEM phase forms an interconnected network. The larger light domains observed likely contain P(LMA-*r*-LiMA) copolymer impurities generated by partial termination of this block during the living synthesis.[27] Their inclusion in the block domains would shift the peak of the SANS data to a lower wavevector, accounting for the discrepancy between periodicities determined by SANS and AFM for this system.

DSC was performed on the three (1:1:1) molar ratio single-ion BCEs in the temperature range of −150 to +150°C. For the triblock system, two distinct T_g values were observed, at −53 and −20°C, thought to correspond to the PLMA and POEM phases, respectively. Thermal signatures for PLiMA should fall outside the temperature range of investigation.[28] The T_g of the POEM block domain (−20°C) is higher than that of POEM homopolymer ($T_g \sim -60$°C), a first indication that Li^+ from the neighboring PLiMA block enters the POEM domains. The DSC trace for PLMA-*b*-P(LiMA-*r*-OEM) similarly reveals two T_g values at −58 and −11°C, indicative of microphase separation. The P(LMA-*r*-LiMA)-*b*-POEM system, by contrast, shows only a single T_g at −12°C. As both SANS and AFM data on this material strongly indicate a microphase-separated structure, the single glass transition may be interpreted as comparable shifts in T_g of the PLMA and POEM domains due to the incorporation of LiMA in the PLMA block, again implying Li^+ migration into adjacent POEM domains.

To verify the single-ion nature of the electrolytes, transference number measurements were made in lithium symmetric cells. Figure 3 shows the current response to the application of a stepped potential to a cell fitted with the PLMA-*b*-PLiMA-*b*-POEM (1:1:1) electrolyte. The current and voltage waveforms are completely in phase,

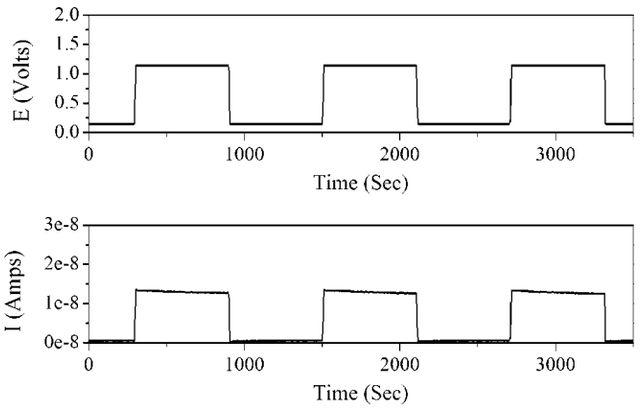

Figure 3. Transference number measurements at room temperature for PLMA-*b*-PLiMA-*b*-POEM (1:1:1) in a lithium symmetric cell.

with no evident polarization. The slight linear decay in the current can be ascribed to the formation and growth of a passivating film on the lithium electrodes; when the magnitude of the applied potential was abruptly reduced to zero, no current behavior akin to a discharging capacitor was observed. Therefore, the anions were effectively immobile over the time frame of the experiment. Longer stepped-potential tests (Fig. 4) demonstrated that anions did not migrate even over a period of several hours. All the electrolytes, including those complexed with BF_3, exhibited similar behavior in stepped-potential studies, indicating that for all materials the transference number was effectively unity.

Figure 5 shows that P(LMA-*r*-LiMA)-*b*-POEM exhibits excellent electrochemical stability at room temperature, with no sign of breakdown evident up to the 5 V limit. This result is consistent with findings published previously.[15] All single-ion systems investigated (including those with BF_3 incorporation) possessed electrochemical stability comparable to that demonstrated in Fig. 5.

AC impedance spectroscopy was used to measure the ionic conductivity of the BCEs over a range of temperatures. Figure 6 displays results for the three systems incorporating equimolar ratios of LiMA, OEM, and LMA in three distinct architectures. Remarkably, the conductivities of the electrolytes with the anion bound outside of the ion-conducting POEM block, namely P(LMA-*r*-LiMA)-*b*-POEM and PLMA-*b*-PLiMA-*b*-POEM, are one to two orders of

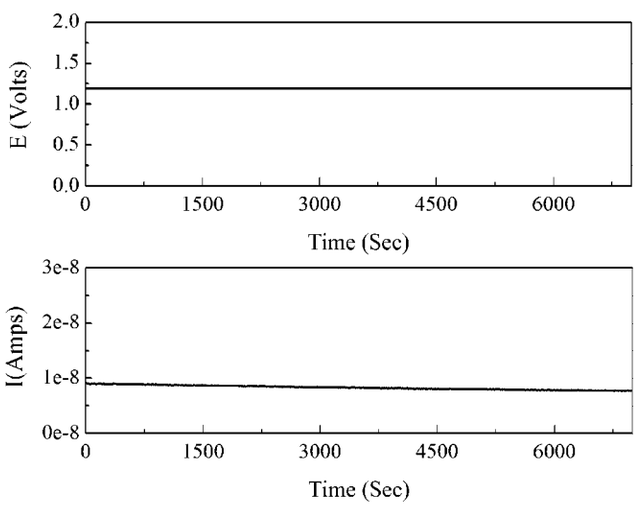

Figure 4. Extended-time transference number measurements at room temperature for PLMA-*b*-PLiMA-*b*-POEM (1:1:1) in a lithium symmetric cell.

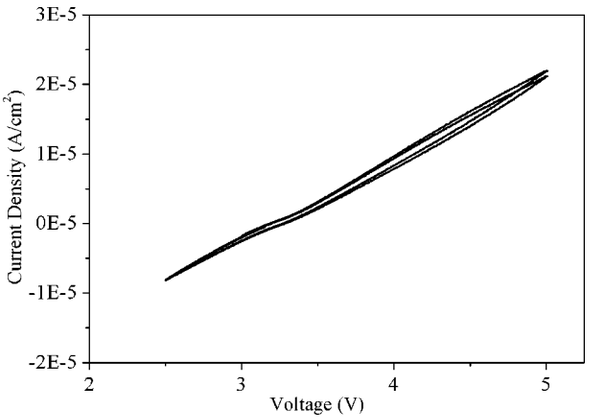

Figure 5. Cyclic voltammetry at room temperature for P(LMA-*r*-LiMA)-*b*-POEM (1:1:1) incorporated in a cell with a platinum working electrode and a lithium counter electrode, demonstrating the electrochemical stability of the single-ion conducting BCE to 5 V. The sweep rate was 25 mV/s.

magnitude higher than that of the PLMA-*b*-P(LiMA-*r*-OEM) material over the range of temperatures studied, confirming preliminary findings by this laboratory.[15] Conductivity data could be fit to the Vogel-Tammann-Fulcher (VTF) equation

$$\sigma = AT^{-1/2} \exp[-E_a/k(T - T_o)] \quad [1]$$

where the pre-exponential term A is proportional to the number of charge carriers in the system, kT is the thermal energy, and T_0 is a reference temperature roughly associated with the T_g of the conducting polymer host. T_o usually falls 25-50 K below T_g. The activation energy, E_a, scales inversely with the ease of motion of the charge carriers. VTF fits (Table III) showed that the variation in conductivity is attributable to vastly different numbers of mobile ions (represented by A). While the activation energy appears to be lowest for PLMA-*b*-P(LiMA-*r*-OEM), any associated gain in conductivity is more than offset by the five order-of-magnitude difference in the pre-exponential A parameter. The VTF fits support the hypothesis that ion dissociation is induced in the P(LMA-*r*-LiMA)-*b*-POEM and PLMA-*b*-PLiMA-*b*-POEM materials by microphase separation

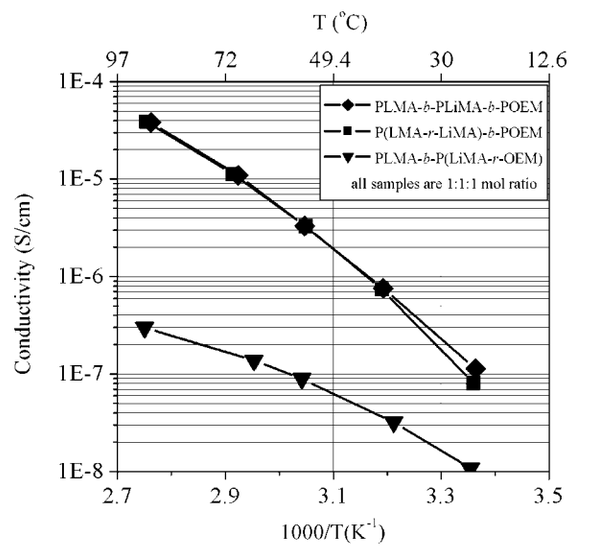

Figure 6. Temperature dependence of electrical conductivity of the single-ion conducting BCEs having 1:1:1 molar ratios LMA:LiMA:OEM. (Anion placement is denoted in the legend.)

Table III. VTF fit parameters for the single-ion BCE materials.

	A ($SK^{0.5}$ cm^{-1})	E_a (eV)	T_o (K)
P(LMA-*r*-LiMA)-*b*-POEM	4.52	0.121	206.2
PLMA-*b*-PLiMA-*b*-POEM	4.82	0.122	205.5
PLMA-*b*-P(LiMA-*r*-OEM)	7.5×10^{-5}	0.026	250.2

of incompatible POEM and PLMA blocks. Upon microphase separation, the anions become spatially isolated from the ion-conducting POEM component, being tethered to the chain backbone. However, the cations are free to migrate into the POEM domains. The recorded conductivities for these systems suggest that the solvating power of PEO for Li^+ is sufficient to overcome the electrostatic energy penalty to separate Li^+ and COO^- into adjacent nanodomains.

Further evidence to this effect is shown in Fig. 7, which compares the FTIR spectra for the P(LMA-*r*-LiMA)-*b*-POEM and PLMA-*b*-P(LiMA-*r*-OEM) systems. The asymmetric stretching vibration of the carboxylate ion is observed at ~1600 cm^{-1} when LiMA is incorporated in the POEM block, as compared to ~1650 cm^{-1} when incorporated in the PLMA block. This shift to higher frequency can be linked to an enhanced dissociation of Li^+ and COO^-. In alkali metal methacrylate homopolymers, this vibration has been reported at ~1560 cm^{-1}.[29] It has further been demonstrated that adding low molecular weight polyethylene glycol (PEG) to random copolymers of methyl methacrylate and LiMA, P(MMA-*r*-LiMA), results in a shift of the COO^- stretch to higher wavenumbers due to ion-dipole interactions between the lithium cations and the ether groups of PEG.[30] In the P(LMA-*r*-LiMA)-*b*-POEM system investigated here, this shift becomes more pronounced, consistent with increased dissociation of Li^+ and COO^-, presumably due to Li^+ migration into the POEM domains.

A more traditional approach to reduce ion pairing in single-ion conducting polymer electrolytes has been to decrease anion charge density, for instance, through the incorporation of a suitable Lewis acid.[12-14] For example, BF_3 has been shown to strongly associate with carboxylate anions, reducing the effective anion charge density and thus ion pairing interactions.[13] When BF_3 was added to the PLMA-*b*-P(OEM-*r*-LiMA) (1:1:1) electrolyte, the conductivity of this material was raised to the level of the other two 1:1:1 systems. The FTIR spectrum of the BF_3-complexed material (Fig. 7) shows a corresponding shift of the asymmetric carboxylate stretch to 1657 cm^{-1}, comparable to the peak position found for P(LMA-*r*-LiMA)-*b*-POEM for this vibration. These findings suggest that BF_3 incorporation induces ion dissociation with effectiveness similar to counter ion isolation. Interestingly, when BF_3 was added to the P(LMA-*r*-LiMA)-*b*-POEM and PLMA-*b*-PLiMA-*b*-POEM (1:1:1) electrolytes, no change in conductivity was observed (Fig. 8). These results support the notion that ion dissociation is already substantially achieved in these systems by the spatial isolation of counter ions resulting from block demixing.

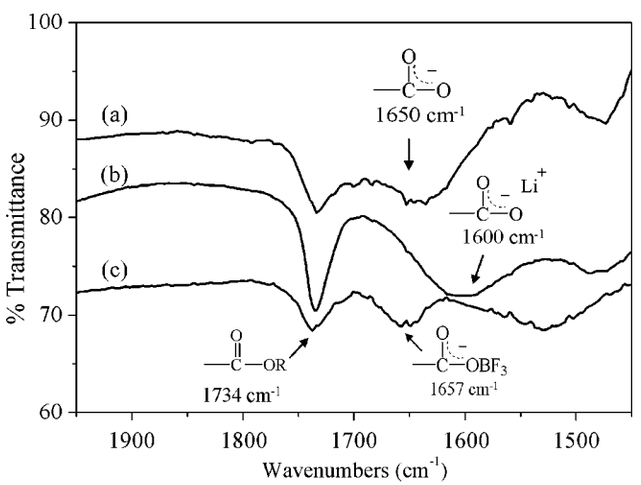

Figure 7. FTIR spectra of single-ion conducting BCEs: (a) P(LMA-*r*-LiMA)-*b*-POEM, (b) PLMA-*b*-P(LiMA-*r*-OEM), and (c) PLMA-*b*-P(LiMA-*r*-OEM) complexed with BF_3.

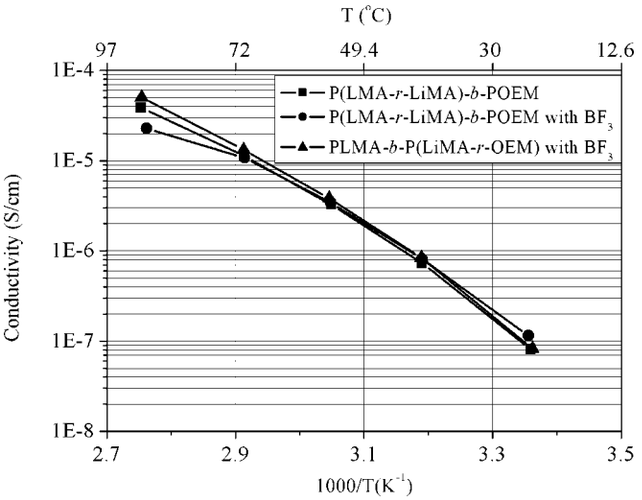

Figure 8. Temperature dependence of electrical conductivity of the single-ion conducting BCEs having 1:1:1 molar ratios LMA:LiMA:OEM after complexation with BF_3.

Although conductivities for the P(LMA-*r*-LiMA)-*b*-POEM and PLMA-*b*-PLiMA-*b*-POEM (1:1:1) systems were an order of magnitude or more above that found for PLMA-*b*-P(LiMA-*r*-OEM) (1:1:1), they remain too low for practical application. For these systems, the relatively high EO:Li ratio of ~9:1 limits the number of unoccupied sites available for Li^+ diffusion, raises the T_g of the polymer, and also possibly induces ion clustering.[31] By diluting the number of charges through a reduction in LiMA content to EO:Li ratios above 20:1, the room temperature conductivity can be appreciably enhanced for both architectures, as shown in Fig. 9. However,

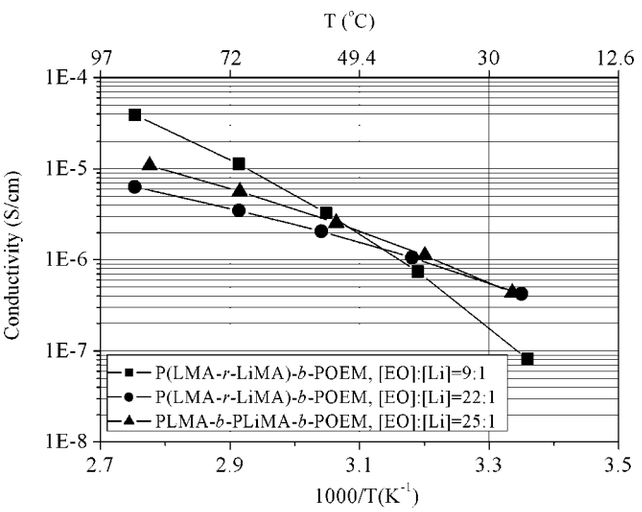

Figure 9. Temperature dependence of electrical conductivity of single-ion conducting BCEs with different EO:Li ratios.

note that having a larger number of charge carriers becomes advantageous at high temperatures, indicating that the optimal architecture for a single-ion conductor depends on the temperature range of the application.

Conclusions

In this work, microphase separation of incompatible PLMA and POEM blocks of single-ion conducting BCEs provided a mechanism to explore the effect of counter ion placement on Li^+ conductivity. When the carboxylate anions were spatially separated from the ion-conducting POEM domains, conductivities were 1 to 2 orders of magnitude higher than for stoichiometrically equivalent materials in which the counter ions resided within the POEM domains. From VTF fits and DSC and FTIR studies, the higher conductivities could be linked to enhanced ion dissociation, apparently due to the migration of Li^+ into POEM. The results imply that the energy gained by Li^+ solvation in POEM is sufficient to outweigh the electrostatic energy penalty for nanoscale separation of Li^+ from COO^-, by rough approximation

$$|E_{Li^+solv}| \geqslant \frac{e^2}{4\pi\epsilon_0\varepsilon r_{Li\text{-}O}} \quad [2]$$

where E_{Li^+solv} is the Li^+ solvation energy, ε is the dielectric constant of P(LMA-*r*-LiMA), and $r_{Li\text{-}O}$ is the distance between Li^+ and O^- in the Li^+-COO^- ion pair. Based on the crystal structure of LiMA,[32] the value of $r_{Li\text{-}O}$ for associated ions can be estimated as 0.20 nm, while ϵ can be conservatively estimated as 2.3 (the value for polyethylene).[33] The required Li^+ solvation energy to achieve ion separation can thus be crudely approximated as ~300 kJ/mol. Recent *ab initio* calculations for Li^+-PEO complexes gave Li^+ binding energies in the range of 500-600 kJ/mol, depending on EO coordination number (4-6),[34] suggesting that Li^+ migration into the POEM domains from PLMA is energetically feasible. This work thus discloses a potential new strategy for enhancing conductivity in single-ion conducting polymer electrolytes by spatial isolation of the counter ion outside of the ion-conducting PEO-based domain.

Acknowledgments

This project has been sponsored by the Office of Naval Research under contracts N00014-99-1-0561, N00014-99-1-0565, and N00014-02-1-0226 and in part by the MIT Materials Research Science & Engineering Centers Program of the National Science Foundation under award DMR-0213282. S.-W.R. acknowledges M. H. Acar for helpful discussions. We acknowledge the support of NIST, U.S. Department of Commerce, in providing the neutron facilities used in this work.

The Massachusetts Institute of Technology assisted in meeting the publication costs of this article.

References

1. P. V. Wright, *MRS Bull.*, **27**, 597 (2002).
2. R. Hooper, L. J. Lyons, D. A. Moline, and R. West, *Silicon Chemistry*, **1**, 121 (2002).
3. M. Doyle, T. F. Fuller, and J. Newman, *Electrochim. Acta*, **39**, 2073 (1994).
4. I. Rey, J. C. Lassegues, P. Baudry, and H. Majastre, *Electrochim. Acta*, **43**, 1539 (1998).
5. Y. Ma, M. Doyle, T. F. Fuller, M. M. Doeff, L. C. De Jonghe, and J. Newman, *J. Electrochem. Soc.*, **142**, 1859 (1995).
6. E. Tsuchida, H. Ohno, and N. Kobayashi, *Macromolecules*, **21**, 96 (1988).
7. Y. Zheng and G. Wan, *J. Macromol. Sci., Pure Appl. Chem.*, **A30**, 365 (1993).
8. R. A. Vaia, S. Vasudevan, W. Krawiec, L. G. Scanlon, and E. P. Giannelis, *Adv. Mater. (Weinheim, Ger.)*, **7**, 154 (1995).
9. T. Fujinami, A. Tokimun, M. A. Mehta, D. F. Shriver, and G. C. Rawsky, *Chem. Mater.*, **9**, 2236 (1997).
10. Y. Tominaga and H. Ohno, *Electrochim. Acta*, **42**, 1561 (1997).
11. J. M. G. Cowie and G. H. Spence, *Solid State Ionics*, **123**, 233 (1999).
12. S.-S. Zhang, Z. Chang, K. Xu, and C. A. Angell, *Electrochim. Acta*, **45**, 1229 (2000).
13. Z. Florjanczyk, W. Bzducha, N. Langwald, J. R. Dygas, F. Krok, and B. Misztal-Faraj, *Electrochim. Acta*, **45**, 3563 (2000).
14. X.-G. Sun, W. Xu, S.-S. Zhang, and C. A. Angell, *J. Phys.: Condens. Matter*, **13**, 8235 (2001).
15. D. R. Sadoway, B. Huang, P. E. Trapa, P. P. Soo, P. Bannerjee, and A. M. Mayes, *J. Power Sources*, **97-98**, 621 (2001).
16. M. Watanabe, H. Tokuda, and S. Muto, *Electrochim. Acta*, **46**, 1487 (2001).
17. X. Ollivrin, F. Alloin, J.-F. LeNest, D. Benrabah, and J.-Y. Sanchez, *Electrochim. Acta*, **48**, 1961 (2003).
18. T. Hirakimoto, M. Nishiura, and M. Watanabe, *Electrochim. Acta*, **46**, 1609 (2001).
19. S. Tabata, T. Hirakimoto, M. Nishiura, and M. Watanabe, *Electrochim. Acta*, **48**, 2105 (2003).
20. P. P. Soo, B. Huang, Y.-L. Jang, Y.-M. Chiang, D. R. Sadoway, and A. M. Mayes, *J. Electrochem. Soc.*, **146**, 32 (1999).
21. A.-V. G. Ruzette, P. P. Soo, D. R. Sadoway, and A. M. Mayes, *J. Electrochem. Soc.*, **148**, A537 (2001).
22. P. E. Trapa, B. Huang, D. R. Sadoway, and A. M. Mayes, *Electrochem. Solid-State Lett.*, **5**, A85 (2002).
23. M. Doyle and J. Newman, *J. Electrochem. Soc.*, **142**, 3465 (1995).
24. J. Evans, C. A. Vincent, and P. G. Bruce, *Polymer*, **28**, 2324 (1987).
25. M. J. Fasolka, P. Banerjee, A. M. Mayes, G. Pickett, and A. C. Balazs, *Macromolecules*, **33**, 5702 (2000).
26. M. J. Fasolka, A. M. Mayes, and S. Magonov, *Ultramicroscopy*, **90**, 21 (2001).
27. T. Pan, K. Huang, A. C. Balazs, M. S. Kunz, A. M. Mayes, and T. P. Russell, *Macromolecules*, **26**, 2860 (1993).
28. E. P. Otocka and T. K. Kwei, *Macromolecules*, **1**, 401 (1968).
29. A. Hamoudi and I. C. McNeill, *Eur. Polym. J.*, **14**, 177 (1978).
30. K.-H. Lee and J.-K. Park, *J. Polym. Sci., Part B: Polym. Phys.*, **36**, 991 (1998).
31. A. Taubert and K. I. Winey, *Macromolecules*, **35**, 7419 (2002).
32. H. P. Beck and P. Trubenbach, *Chem. Ber.*, **125**, 613 (1992).
33. *Polymer Handbook*, 3rd ed., J. Brandrup and E. H. Immergut, Editors, Wiley Interscience, New York (1989).
34. P. Johansson, *Polymer*, **42**, 4367 (2001).